

Effects of Yb addition on microstructures and mechanical properties of 2519A aluminum alloy plate

ZHANG Xin-ming(张新明), WANG Wen-tao(王文韬), CHEN Ming-an(陈明安), GAO Zhi-guo(高志国),
JIA Yu-zhen(贾寓真), YE Ling-ying(叶凌英), ZHENG Da-wei(郑大伟),
LIU Ling(刘玲), KUANG Xiao-yue(匡小月)

School of Materials Science and Engineering, Central South University, Changsha 410083, China

Received 29 June 2009; accepted 25 August 2009

Abstract: The effects of Yb content on the microstructures and mechanical properties of 2519A aluminum alloy plate were investigated by means of tensile test, optical microscopy, transmission electron microscopy, scanning electron microscopy and X-ray diffractometer. The results show that addition of 0.17% (mass fraction) Yb increases the density of θ' particles of the 2519A alloy plate and reduces the coarsening speed rate of θ' phase at 300 °C. Therefore, tensile strength is enhanced from 483.2 MPa to 501.0 MPa at room temperature and is improved from 139.5 MPa to 169.4 MPa at 300 °C. The results also show that with the addition of 0.30% (mass fraction) Yb, the mechanical properties increase at 300 °C and decrease at room temperature. With Yb additions, the $Al_{7.4}Cu_{9.6}Yb_2$ phase is found whilst the segregated phases of as-cast alloys along grain boundaries become discontinuous, thin and spheroidized.

Key words: rare-earth; ytterbium; 2519A aluminum alloy; microstructure; tensile properties

1 Introduction

High-strength 2519 aluminum alloy is primary material for many applications, such as military aircrafts, helicopters and amphibious[1–2]. 2519A alloy with higher Cu/Mg ratio has superior mechanical properties, weldability and stress corrosion cracking resistance[3–5]. But it is necessary to further improve the mechanical properties, especially those at elevated temperature, to enhance the high ballistic resistance.

It is well known that trace element additions to aluminum alloys can strongly influence the precipitation process, including modifying the dispersion, morphology and crystal structure of the resulting precipitations[6–8]. Studies on rare-earths as micro-alloying elements showed that they had beneficial effects on the mechanical properties of aluminum alloys. It was reported that addition of Ce to Al-Cu-Mg-Ag alloy improved the thermal stability of the Ω phase thus raised the service temperature of this alloy[9]. LI et al[10] demonstrated that adding 0.1%–0.2% (mass fraction) Y improved the tensile properties of 2519 alloy at room and elevated temperatures for Y changed the size and density

of θ' phase. It was indicated that Nd was mainly distributed in form of intermediate compound AlCuNd, which exerted a restraining force on the grain boundaries and enhanced the mechanical properties of 2519 alloy at high temperature[11].

Some recent researches showed that Yb was considered as an effective micro-alloying element in aluminum alloys. It was reported that Yb addition improved the mechanical properties of Al-Cu-Mg-Ag alloy and Al-Zn-Mg-Cu-Zr alloy[12–13]. Furthermore, complex additions of Yb, Cr and Zr to Al-Zn-Mg-Cu alloy significantly enhanced the resistance to recrystallization[14]. The present work was to examine such effect of Yb addition on 2519A aluminum alloy plate in order to explore the potential for enhancing its mechanical properties.

2 Experimental

Table 1 lists the chemical compositions of the studied alloys with Yb additions of 0%, 0.17% and 0.30% (mass fraction). Al-Mn, Al-Yb, Al-Zr, Al-Ti-B master alloys, commercial Mg, Cu and Al were used to prepare the alloys in an induction furnace. The alloys

were melted at 780 °C, degassed for 10–15 min by adding C_2Cl_6 , and then cast into iron moulds to produce billets in a size of 100 mm×100 mm×25 mm. The billets were homogenized at 530 °C for 24 h, followed by air cooling, and then hot-rolled to 2.4 mm in thickness. Subsequently, the plates were solution-treated at 535 °C for 2 h, water-quenched, and finally peak aged at 165 °C with prior cold-rolled reduction of 15% (T8 temper). The aging times for alloys 1, 2 and 3 were 14, 13 and 12 h, respectively.

Table 1 Chemical compositions of experimental alloys (mass fraction, %)

Alloys	Cu	Mn	Mg	Ti	Zr	Yb	Al
1	5.79	0.31	0.20	0.04	0.28	0.00	Bal.
2	5.75	0.32	0.21	0.04	0.22	0.17	Bal.
3	5.82	0.31	0.21	0.05	0.24	0.30	Bal.

Tensile measurements were performed on CSS-44100 and RWS 50 machines for room temperature tests and high temperatures tests, respectively. The specimens used were T8 tempered and the stretching speeds for the two tests were both 2 mm/min. In the tests at high temperatures, the specimens were held at 300 °C and 400 °C for 10 min, respectively, to achieve thermal equilibration. The mechanical results reported in this study were the mean values of at least two specimens.

The X-ray diffraction pattern (XRD) was recorded on the D/max 2500 X-Ray diffractometer. The microstructures of the studied alloys were analyzed on the Sirion 200 scanning electron microscope (SEM) and the Tecnai G² 20 transmission electron microscope (TEM). TEM samples were electro-polished in a 70% ethanol and 30% (volume fraction) nitric acid solution at -20°C, using a twin-jet equipment operated at 20 V.

3 Results

3.1 As-cast microstructures

The as-cast microstructures of the alloys with different Yb additions are shown in Fig.1. Obviously, the grain boundaries are changed by adding Yb. Without Yb, the segregated phases of the alloy 1 (Fig.1(a)) are continuous and coarse which present a reticular formation along grain boundaries composed of Al_2Cu , Al_7Cu_2Fe and $\alpha(Al)$ phases. However, with addition of 0.17% Yb, these compounds along grain boundaries become discontinuous and thin (Fig.1(b)). With the increase of Yb addition, the segregated phases are more discontinuous, and some spherical particles can be observed in the alloy 3 (Fig.1(c)). According to the results of EDS attached to SEM, these spherical particles are rich in Al, Cu and Yb (Table 2).

The XRD results of the as-cast specimens are shown in Fig.2. With Yb addition, a new phase of

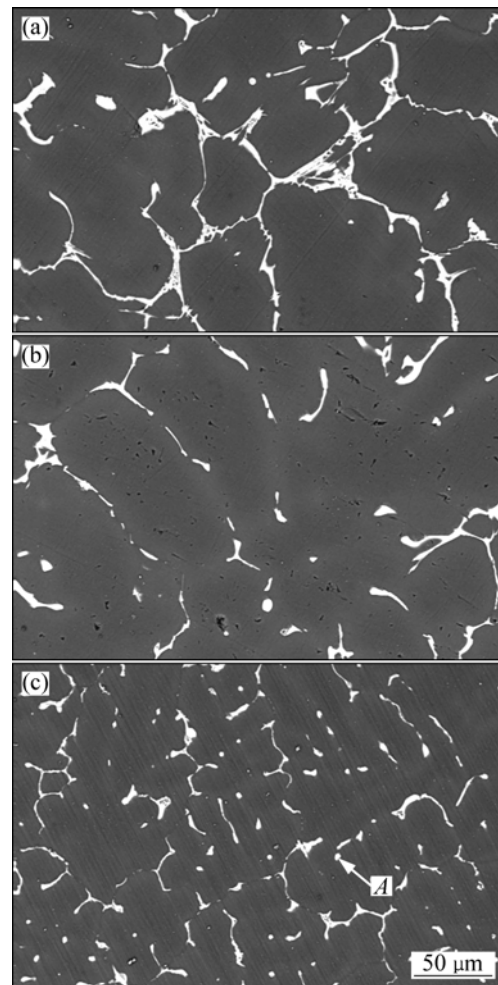


Fig.1 SEM images of as-cast microstructures: (a) Alloy 1; (b) Alloy 2; (c) Alloy 3

Table 2 EDS results of position A in Fig.1(c)

Element	w/%	x/%
Al	50.46	71.27
Yb	2.61	0.58
Cu	46.93	20.15

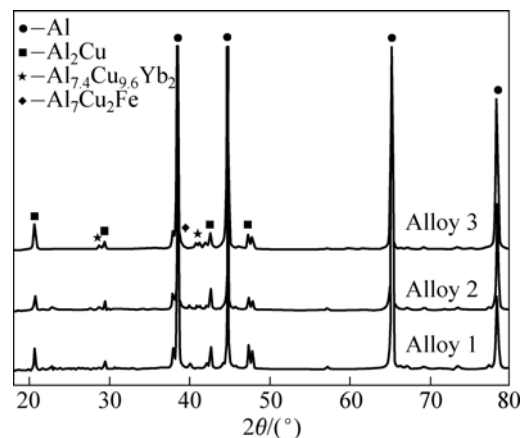


Fig.2 XRD patterns of specimens

$Al_{7.4}Cu_{9.6}Yb_2$ appears in alloy 2 and alloy 3. Meanwhile the height of the Al_7Cu_2Fe phase peak becomes lower with increasing Yb content, this peak even disappears when Yb content reaches 0.30%, which indicates that Yb reduces the content of the impurity.

3.2 Microstructures and mechanical properties of peak-aged alloy plates (T8 temper)

The tensile properties of the studied alloy plates of T8 temper at various test temperatures are listed in Table 3. The results show that the tensile strength at room temperature increases from 483.2 MPa to 501.0 MPa when the Yb content increases from 0% to 0.17%. But it decreases gradually when Yb content rises from 0.17% to 0.30%. At 300 °C, the tensile strength is improved from 139.5 MPa to 169.4 MPa and 155.5 MPa correspondingly when adding 0.17% and 0.30% Yb, respectively. The tensile strengths of the alloys 1, 2 and 3 at 400 °C are 42.1, 41.0 and 45.2 MPa, respectively, which shows that Yb has little effect on the mechanical properties at 400 °C.

With different Yb contents, the elongations of the alloy plates change appreciably. Adding 0.30% Yb, the elongation decreases from 10.8% to 10.5% at room temperature, from 22.1% to 21.2% at 300 °C and from 65.0% to 62.0% at 400 °C, respectively. It can be concluded that 0.17% Yb addition increases the tensile strength at room temperature and 300 °C, but slightly decreases the elongation.

The microstructures of the studied alloy plates 1, 2 and 3 were investigated by TEM. Fig.3 shows the TEM

images of the alloy plates peak-aged at 165 °C. It can be seen from Fig.2 that the dominant phase θ' precipitates, as platelets on the $\{001\}$ Al plane, are uniformly distributed in the grains of three alloys (Figs.3(a–c)). Compared with the Yb-free alloy, the density of θ' phase is higher in alloy 2 with 0.17% Yb addition. However, when the content of Yb increases to 0.30%, the density of θ' phase decreases. Meanwhile, the second phases distributed along grain boundaries in alloy 2 are finer and more uniform than those in the plates of alloys 1 and 3.

To further understand the difference of θ' phase in intrinsic feature at high temperature, the peak-aged alloys were thermal insulated at 300 °C for 10 min and then stretched. Fig.4 shows the θ' phase coarsened in the grains of three alloys. Obviously, the θ' precipitates in alloy 2 are more densely distributed than those in alloy 1,

Table 3 Mechanical properties of alloy plates at different temperatures

Alloy	Testing temperature/°C	Tensile strength/MPa	Elongation/%
1 (0%Yb)	25	483.2	10.8
	300	139.5	22.1
	400	42.1	65.0
2 (0.17%Yb)	25	501.0	10.7
	300	169.4	21.0
	400	41.0	62.6
3 (0.30%Yb)	25	469.4	10.5
	300	155.5	21.2
	400	45.2	62.0

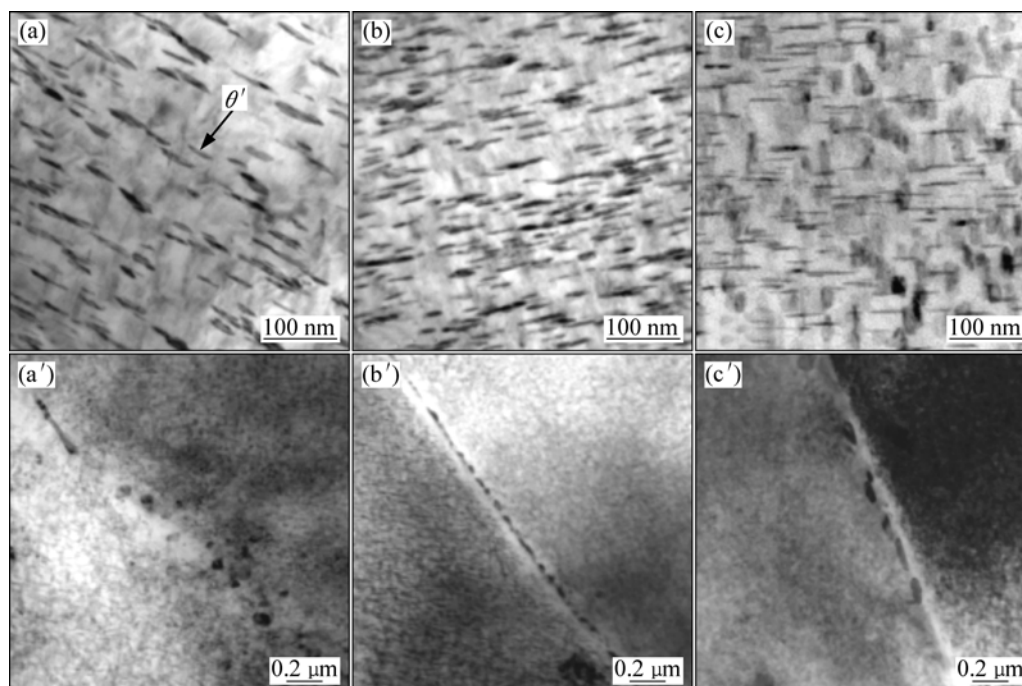


Fig.3 TEM micrographs of peak-aged alloy plates: (a), (a') Alloy 1; (b), (b') Alloy 2; (c), (c') Alloy 3

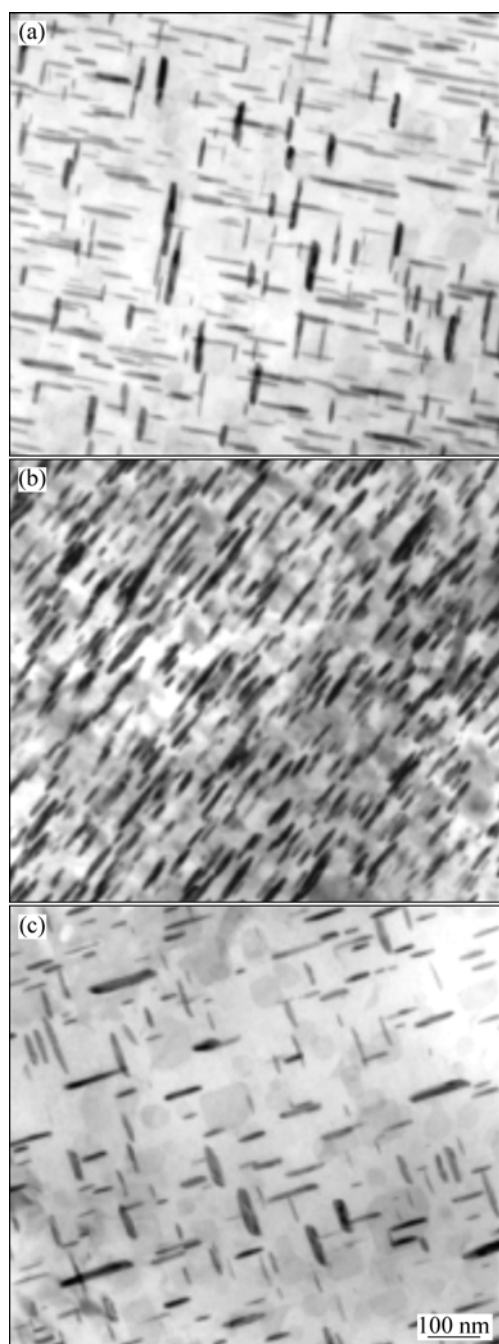


Fig.4 TEM micrographs of alloy plates stretched at 300°C: (a) Alloy 1; (b) Alloy 2; (c) Alloy 3

whereas the amount of θ' in alloy 3 is the least.

4 Discussion

The present work shows that the addition of Yb obviously affects the microstructures and mechanical properties of 2519A aluminum alloy plate of T8 temper. With addition of Yb, the size and density of the predominant hardening precipitates, θ' phase, are changed. The θ' phase in the alloy plate with addition of 0.17% Yb is the densest, the tensile strength of which is

thus the highest. The diameter of Yb atom, 0.194nm, is larger than that of Al atom (0.143 nm), so when it enters the matrix, it will certainly cause great lattice distortion and increase system energy. In order to keep low system energy, there is more oversaturated vacancies aggregating around Yb atoms. Consequently, it is liable for θ' phase to nucleate at dislocation and vacancy cluster since θ' phase is semi-coherent with Al matrix[15]. In addition, lattice distortion energy and vacancy energy increased by Yb atom provide driving force. As a result, it is beneficial for θ' phase to nucleate near Yb atom, which might be the reason that Yb increases the density of θ' phase. Moreover, the second phases distributed on the grain boundaries in the alloy 2 are finer and more uniform, which strengthens the grain boundaries. That is another factor that 0.17% Yb addition improves the tensile strength. However, 0.30% addition of Yb decreases the strength because excessive Yb atoms form the Yb containing intermediate compounds with Al and Cu atoms. Consequently, the solid solubility of Cu in Al is reduced and the precipitation of θ' phase is limited accordingly.

At 300 °C, the density of θ' phase in alloy 2 with 0.17% Yb is the highest apparently and the size of θ' phase is the smallest (Fig.4), Hence the mechanical properties of the plate of alloy 2 at 300 °C are the highest. With addition of Yb, the diffusion of Cu may be restrained by large Yb atoms which are aggregated by vacancy clusters. Therefore, the coarsening speed rate of the θ' phase reduces, and the tensile strength of the Yb containing alloy plates is thus increased at elevated temperature.

The SEM images and XRD results of the as-cast alloys show that the remnant Al_2Cu phase decreases with the increase of Yb addition. Since some of Cu forms the compound of AlCuYb which might be $\text{Al}_{7.4}\text{Cu}_{9.6}\text{Yb}_2$ phase, the solid solubility of Cu in Al is reduced. As a result, the remnant Al_2Cu dissolved along the grain boundaries decreases correspondingly and causes the grain boundaries of Yb containing alloys become thin and discontinuous (Fig.1). It is inferred that Yb containing alloys with such as-cast microstructures may have good plasticity and workability.

5 Conclusions

1) Addition of 0.17% Yb to 2519A aluminum alloy plate induces the precipitation of finer and denser θ' phase compared with the Yb-free alloy. The tensile strength of T8 temper alloy is thus increased by 17.8 MPa.

2) Addition of Yb up to 0.30% increases the density and reduces the coarsening speed rate of θ' phase at 300 °C, which improves the thermal stability of 2519A

aluminum alloy plate at high temperature up to 300 °C.

3) With addition of Yb, the $Al_{7.4}Cu_{9.6}Yb_2$ phase is observed, while the segregated phases of the as-cast microstructure along grain boundaries, including remnant Al_2Cu , $Al_{7.4}Cu_{9.6}Yb_2$ and $Al_{7.4}Cu_{9.6}Yb_2$ phases, become discontinuous, thin and spheroidized.

References

- [1] FISHER J J Jr, KRAMER L S, PICKENS J R. Aluminum alloy 2519 in military vehicles [J]. *Advanced Materials and Processes*, 2002, 160 (9): 43–46.
- [2] DYMEK S, DOLLAR M. TEM investigation of age-hardenable Al 2519 alloy subjected to stress corrosion cracking tests [J]. *Materials Chemistry and Physics*, 2003, 81(2/3): 286–288.
- [3] GAO Z G, ZHANG X M, CHEN M A. Influence of strain rate on the precipitate microstructure in impacted aluminum alloy [J]. *Scripta Materialia*, 2008, 59: 983–986.
- [4] GAO Z G, ZHANG X M, CHEN M A. Investigation on θ' precipitate thickening in 2519A-T87 aluminum alloy plate impacted [J]. *Journal of Alloys and Compounds*, 2009, 476: L1–L3.
- [5] ZHANG X M, LI H J, LI H Z, GAO H, GAO Z G, LIU Y, LIU B. Dynamic property evaluation of aluminum alloy 2519A by split Hopkinson pressure bar [J]. *Transactions of Nonferrous Metals Society of China*, 2008, 18(1): 1–5.
- [6] SOFYAN B T, RAVIPRASAD K, RINGER S P. Effects of microalloying with Cd and Ag on the precipitation process of Al-4Cu-0.3Mg(wt %) alloy at 200 °C [J]. *Micron*, 2001, 32: 851–856.
- [7] RINGER S P, HONO K, POLMEAR I J, SAKURAL T. Nucleation of precipitation in aged Al-Cu-Mg-(Ag) alloys with high Cu: Mg ratios [J]. *Acta Materialia*, 1996, 44(5): 1883–1898.
- [8] BARLAT F, LIU J. Precipitate-induced anisotropy in binary Al-Cu alloys [J]. *Materials Science and Engineering A*, 1998, 257: 47–61.
- [9] XIAO D H, WANG J N, DING D Y, YANG H L. Effect of rare earth Ce addition on the microstructure and mechanical properties of an Al-Cu-Mg-Ag alloy [J]. *Journal of Alloys and Compounds*, 2003, 352: 84–88.
- [10] LI H Z, LING X P, LI F F, GUO F F, LI Z, ZHANG X M. Effect of Y on microstructure and mechanical properties of 2519 aluminum alloy [J]. *Transaction of Nonferrous Metals Society of China*, 2007, 17(6): 1191–1198.
- [11] ZHANG X M, WANG W T, LIU B, CHEN M A, LIU Y, GAO Z G, YE L Y, JIA Y Z. Effect of Nd addition on microstructures and heat-resisting properties of 2519 aluminum alloy [J]. *The Chinese Journal of Nonferrous Metals*, 2009, 19(1): 15–20. (in Chinese)
- [12] XIAO D H, HUANG B Y. Effect of Yb addition on precipitation and microstructure of Al-Cu-Mg-Ag alloys [J]. *Transactions of Nonferrous Metals Society of China*, 2007, 17(6): 1181–1185.
- [13] FANG H C, CHEN K H, ZHANG Z, ZHU C J. Effect of Yb addition on microstructures and properties of 7A60 aluminum alloy [J]. *Transactions of Nonferrous Metals Society of China*, 2008, 18(1): 28–32.
- [14] CHEN K H, FANG H C, ZHANG Z, CHEN X, LIU G. Effect of Yb, Cr and Zr additions on recrystallization and corrosion resistance of Al-Zn-Mg-Cu alloys [J]. *Materials Science and Engineering A*, 2008, 497: 426–431.
- [15] VAITHYANATHAN V, WOLVERTON C, CHEN L Q. Multiscale modeling of θ' precipitation in Al-Cu binary alloys [J]. *Acta Materialia*, 2004, 52: 2973–2987.

(Edited by FANG Jing-hua)